UNIVERSITÀ DI TRENTO

PROJECT REPORT

Mathematical modeling and simulation

Stochastic representations of ion channel kinetics and exact stochastic simulation of neuronal dynamics

Giacomo Fantoni and Alessandro Polignano

Date: 14 02 2023

Abstract

In this report we present a number of models describing neuronal dynamics. Firstly we present a simple leaky integrate-and-fire model, a fully deterministic representation of the neuron, which equates it to a single resistance-capacitance circuit. The ability of generating spikes in this model is hard coded posing a threshold on the membrane potential. This model is then expanded as to model supra-threshold dynamics, adding to the model a new state variable, the inter-spike time, allowing to model time-dependent changes in the systems parameter. The deterministic model is expanded again to model spike-rate adaptation and synaptic transmission. The deterministic representation of the model doesn't allow to explore channels opening and closing, so we introduce a piecewise stochastic representation for the model. The neuron is then modelled as an hybrid system in which the voltage evolves deterministically in between stochastic channel events. We implemented two representation for the stochastic model: the random time change and Gillespie's direct method. Finally we explored how these two representation differs and propose a methodology to fit them to experimental data.

1. Introduction

Fluctuations in membrane potential arise in part due to stochastic switching in voltage-gated ion channel populations. Neural dynamics is represented by a stochastic model, with noise arising through the molecular fluctuations of ion channel states. Nerve cells are represented by a single isopotential volume surrounded by a membrane with capacitance $C > 0$. These are hybrid stochastic models which include continuous and piecewise differentiable components. These components are coupled: the parameters of the ordinary differential equation for the voltage depend upon the number of open channels, and the propensity of state transition of the channels depend on the voltage.

These hybrid stochastic models are described in the literature by providing and ODE governing the continuous portion of the system and a chemical master equation providing the dynamics of the probability distribution of the jump portion. These models are piecewise-deterministic Markov processes or PDMP, which can be charaterized by providing:

- The ODE for the absolutely continuous portion of the system.
- A rate function that determines when the next jump of the process occurs and a transition measure determining which type of jump occurs at that time.

The use of the PDMP formalism allowed the formulation of limit theorems, dimensionality reduction schemes and extensions of the models to the spatial domain.

1.1 Deterministic neural dynamics model

Deterministic neuronal dynamics models abstract from the channel states and evolve only according to a set of ordinary differential equations. This type of model is described in [2] and encompasses four characteristics of neuronal activity:

- Neurons are Dynamic units.
- Neurons are driven by stochastic forces.
- Neurons are organized into population with similar biophysical properties and response characteristics.
- Multiple populations interact to form functional networks.

To build a neural model the starting point is a deterministic characterization of neurons. In particular, their response to an input $s(t)$ has a generic form represented as:

$$\frac{\partial x}{\partial t} = f(x(t), s(t), \theta) \tag{1}$$

Where x is the state vector that defines a space within which its dynamics unfold. The dimensionality of the space depends depends on the variables of x, which will be the membrane potential and the proportion of open ionic channels. The solution of equation 1 will be the trajectory in time of a point in $x \in x(t)$. The right-hand term is a function of:

- The states $x(t)$.
- The input $s(t)$, exogenous or internal.
- The model parameters θ, the time-constant characteristics of the system.

As neurons are electrical units they can be represented as a resistance-capacitance circuit, for which the voltage evolves according to:

$$C\frac{dV}{dt} = \sum_i I_i(t)$$

Where:

- V is the membrane potential.
- C is the membrane capacitance.
- I_i the membrane current from source i.

The dynamic repertoire of a specific model depends on the nature of the different source currents, which can include fixed-point attractors, limit cycles and chaotic dynamics.

1.1.1 Leaky integrate-and-fire

The easiest model is the simple integrate-and-fire model, where all voltage and synaptic channels are ignored: the current is modelled as a constant passive leak of charge, reducing the equation to:

$$C\frac{dV}{dt} = g_L(E_L - V) + s(t)$$

Where:

- g_L is the conductance of the leak current.
- E_L is equilibrium potential.

This model does not model the biophysical properties necessary for spike generation. Instead spiking is modelled as a threshold process: once the membrane potential exceed the threshold value V_T a spike is assumed and the membrane potential is reset to a resting value V_R, such that $V_R \leq E_L \leq V_T$. No spike is actually emitted and only sub-threshold dynamics are modelled. So, in conclusion the models behave according to:

$$\begin{cases} C\frac{dV}{dt} = g_L(E_L - V) + s(t) & V < V_T \\ V = V_R & V \geq V_T \end{cases}$$

We implemented it solving the system with the forward Euler method for $100s$ of total simulation. The parameters used were:

- Time step $0.0002s$.
- $E_l = -73mV$.
- $V(0) = -73mV$.
- $g_L = 0.025\mu S$.
- $C = 0.375nF$.
- $V_T = -53mV$.
- $V_R = -90$.

As described in [2]. The trajectory obtained is visible in figure 1.

The input current $s(t)$ was studied ad hoc to try to characterize at best the behaviour of the system. We applied impulses for one time step of three different intensities such that:

1. One impulse was enough to generate a spike.
2. More impulses had to cooperate to generate a spike.
3. The impulses would not be able to generate a spike but would make the voltage oscillate around a point greater than E_L.

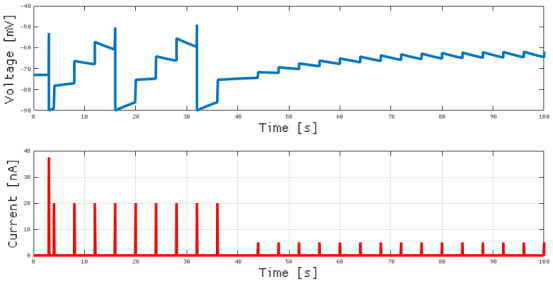

Figure 1. Trajectory of the leaky integrate-and-fire neuronal model. **Top** The membrane voltage. **Bottom** The input current.

1.1.2 Modelling supra-threshold dynamics

To allow the system to generate spikes the integrate and fire model is augmented with an additional variable T, the inter-spike time or IST. This will be modelled as a state variable because:

- It constraints the neuronal trajectory to a finite region of the state space.
- The time between spikes can bee computed directly from its density.
- It allows to model time-dependent changes in the systems parameters.

The resulting model is two-dimensional and automates renewal to reset voltage once the threshold has been exceeded.

$$\begin{aligned} \frac{dV}{dt} &= \frac{1}{C}(g_L(E_L - V) + s(t)) + \alpha(V_R - V)\beta \\ \frac{dT}{dt} &= 1 - \alpha T H(V) \\ \beta &= e^{-\frac{T^2}{2\gamma^2}} \\ H(V) &= \begin{cases} 1 & V \geq V_T \\ 0 & V < V_t \end{cases} \end{aligned} \tag{2}$$

A feature of this model is that the input has to reach a threshold before spikes are generated. After this threshold the firing rate increases monotonically. The membrane voltage is reset to V_R using the Heaviside function H, ensuring that once $V > V_T$, the rate of change of T is large and negative (typically $\alpha \approx 10^4$), reversing the progression of the IST back to zero. After that it will increase constantly for $V_R < V < V_T$. The membrane potential is coupled to T via the Gaussian factor β, centred at $T = 0$ and with a small dispersion $\gamma = 1ms$. During the first few millisecond this term provides a brief impulse to clam the membrane potential near to V_R modelling the refractory period. We implemented this model in Matlab solving the system of equation with the variable order method *ode15s*, expanding the parameter of the leaky integrate and fire with:

- $alpha = 10^4$.
- $gamma = 1ms$.
- $V_0 = -73mV$.
- $T_0 = 0$.

Again the current was built ad hoc as to explore at best model's dynamics. The trajectory of the neuron can be seen in figure 2.

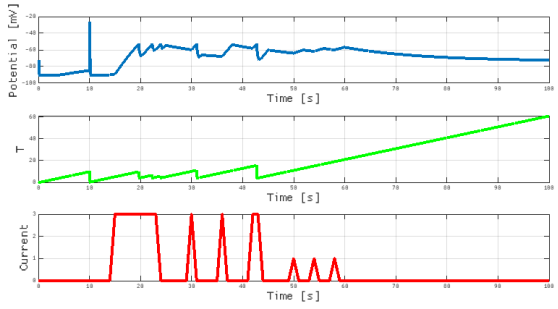

Figure 2. Trajectory of the supra-threshold model. **Top** Membrane voltage, **Middle** Inter spike time. **Bottom** Input current.

It can be seen how the inter spike time goes quickly to zero whenever the membrane voltage crosses the threshold, causing it to go quickly to V_R.

1.1.3 Modelling spike-rate adaptation and synaptic dynamics

Equation 2 can be extended to include ion-channel dynamics to model spike-rate adaptation and synaptic transmission:

$$\begin{aligned}
\frac{dV}{dt} &= \frac{1}{C}\Bigg(g_L(E_L - V) + g_{sK}x_{sK}(E_{sK} - V) + \\
&+ g_{AMPA}x_{AMPA}(E_{AMPA} - V) + \\
&+ g_{GABA}x_{GABA}(E_{GABA} - V) + \\
&+ \frac{g_{NMDA}x_{NMDA}(E_{NMDA} - V)}{1 + e^{-\frac{V-a}{b}}}\Bigg) + \\
&+ \alpha(V_R - V)\beta \\
\frac{dT}{dt} &= -\alpha TH(V) \\
\tau_{sK}\frac{dx_{sK}}{dt} &= (1 - x_{sK})4\beta - x_{sK} \\
\tau_{AMPA}\frac{dx_{AMPA}}{dt} &= (1 - x_{AMPA})(p_{AMPA} + s(t)) - x_{AMPA} \\
\tau_{GABA}\frac{dx_{GABA}}{dt} &= (1 - x_{GABA})p_{GABA} - x_{GABA} \\
\tau_{NMDA}\frac{dx_{NMDA}}{dt} &= (1 - x_{NMDA})p_{NMDA} - x_{NMDA}
\end{aligned} \tag{3}$$

In this way spike-rate adaptation and synaptic dynamics are modelled by a generic synaptic channel mechanism, considering:

- Fast excitatory AMPA channels.
- Slow excitatory NMDA channels.
- Inhibitory GABA channels.
- Slow potassium channels.

Where x_i is the activation variable that controls the proportion of open channels and in particular $0 \leq x_i \leq 1$. Given no input, the ratio of open to closed channel will relax to the equilibrium state:

$$\frac{p}{1+p}$$

For GABA and NMDA channels.

The rate of closing is proportional to x_i, while the rate of opening will be proportional to $1 - x_i$. Synaptic inputs is taken in consideration by increasing the opening rate of AMPA channels instead of affecting V directly. We implemented this model with the same variable order method *ode15s* in Matlab as the supra-threshold one, adding to its parameters:

- $g_sk = 0.128nS$.
- $g_ampa = 0.024nS$.
- $g_gaba = 0.064nS$.
- $g_nmda = 0.08nS$.
- $E_sk = -90mV$.
- $E_ampa = 0mV$.
- $E_gaba = -70mV$.
- $E_nmda = 0mV$.
- $p_ampa = 0.875$.
- $p_gaba = 0.0625$.
- $p_nmda = 0.0625$.
- $tau_ampa = 2.4ms$.
- $tau_gaba = 7ms$.
- $tau_nmda = 100ms$.
- $tau_sk = 80ms$.
- $a = -53$.
- $b = 100$.

The trajectory can be seen in **??**.

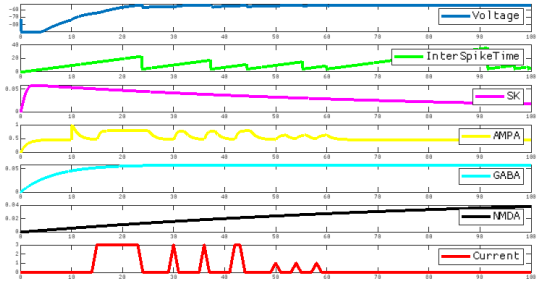

Figure 3. Trajectory of the synaptic dynamics model. From top to bottom **1** Membrane voltage, **2** Inter spike time. **3** Percentage of open Potassium channels. **4** Percentage of open AMPA channels. **5** Percentage of open GABA channels. **6** Percentage of open NMDA channels. **7** Input current.

It can be seen from this how T behave as previously, while the state of the channels cause a different response as before. In particular it can be seen how the fast AMPA channel (in yellow) respond quickly to an input current, while the other have a slower behaviour that cannot be fully characterized in the limited simulation time. This model is useful because it allows the neuron to respond differently based on its history, coupling it with the activity of other neurons in the network, which would cause to change its dynamics.

1.1.4 Introducing noise to the leaky integrate and fire model

The addition of system noise in the form of a random input will transform the deterministic equation into a stochastic differential equation or SDE or Langevin equation. This type of equation has an ensemble of solutions. The effect of the variable spike-time arrival disperse trajectories through the state space. Going back to the system described by equation 1, with $s(t)$ as a random variable:

$$s(t) = h \sum_n \delta(t - t_n) \tag{4}$$

Where:

- h is a discrete quantity representing the change in post-synaptic membrane potential due to a synaptic event.
- t_n represents the time of the n-th event.

Typically the time between spikes is sampled from a Poisson distribution. Given the neuronal response function $\sigma(t)$, the mean impulse rate $r(t)$ can be computed by taking an average over a short time-interval T:

$$\begin{aligned} \sigma(t) &= \sum_n \delta(t - t_n) \\ r(t) &= \frac{1}{T} \int_0^T \sigma(\tau) d\tau \\ s(t) &= hr(t) \end{aligned} \tag{5}$$

We then simulated the leaky fire and integrated model with and s built such that:

$$s(t) \begin{cases} 20nA & t \in \mathcal{I} \\ 0 & otherwise \end{cases}$$

Where $\mathcal{I}$ contains the time of firing t_i sampled from a Poisson distribution with $\lambda = 10$. A trajectory example can be seen in 4

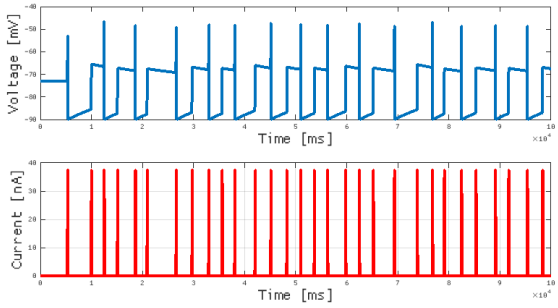

Figure 4. Trajectory of the leaky integrate-and-fire neuronal model with stochastic input current. **Top** The membrane voltage. **Bottom** The input current.

We then simulated it for 1000 seconds to compute the mean impulse rate, which was averaged over 10 independent runs, obtaining:

$$\bar{r}(t) = 0.083$$

1.2 Expanding the stochastic neuronal model

In this paper two piecewise stochastic representations for the models are introduced. In this representations the noise arise via stochastic counting processes. These representations imply different exact simulation strategies, which are not being explored in this context. From a computational standpoint the change to path wise representation is useful because:

- The different representations imply different exact simulation strategies.
- The different representation can be used to develop new methods such as finite difference methods for the approximation of parametric sensitivities and multilevel Monte Carlo methods for the approximation of expectations.
- The representations can be used for the rigorous analysis of different computational strategies and for the algorithmic reduction of models with multiple scales.

These representations are not well known in the context of computational neuroscience and so approximated methods for the simulation of sample paths like fixed time step methods or piecewise constant propensity algorithm are still used in the literature where there is no need to make such approximations. Because of this this work should contribute in a way to:

- Formulate two pathwise representations for the specific models under consideration.
- A presentation of the corresponding exact simulation strategies for the different representations.
- A comparison of the two strategies applied on the Morris-Lecar model.

Moreover this work show how to use the different representations in the development of methods for parametric sensitivity analysis.

2. Stochastic representations

2.1 Random time change representation

Consider a model of a system with states A for closed and B for open of an ion channel. The dynamics of the system are modelled assuming that the dwell times in the two states are determined by independent exponential random variables with parameters α and β:

$$A \underset{\beta}{\overset{\alpha}{\rightleftharpoons}} B$$

The probability that a closed channel opens in the next increment of time Δs is assumed $\alpha \Delta s + o(\Delta s)$, while the probability that an open channel closes is assumed $\beta \Delta s + o(\Delta s)$. This model can be described mathematically by a chemical master equation, that for the two states model is:

$$\begin{cases} \frac{d}{dt} p_{x_0}(A, t) = -\alpha p_{x_0}(A, t) + \beta p_{x_0}(B, t) \\ \frac{d}{dt} p_{x_0}(B, t) = -\beta p_{x_0}(B, t) + \alpha p_{x_0}(A, t) \end{cases}$$

Where:

- $p_{x_0}(x,t)$ is the probability of being in state $x \in \{A,B\}$ at time t given the initial condition x_0.
- x_0 is the initial condition.

The chemical master equation is a linear ODE governing the dynamical behaviour of the probability distribution of the model and does not provide a stochastic representation for a particular realization of the process. To reconstruct a path-wise representation let:

- $R_1(t)$ be the number of times $A \to B$ has taken place by time t.
- $R_2(t)$ be the number of times $B \to A$ has taken place by time t.
- $X_1(t) \in \{0,1\}$ be 1 if the channel is closed at time t and zero otherwise.
- $X_2(t) = 1 - X_1(t)$ be 1 if the channel is open at time t and zero otherwise.
- $X(t) = \begin{pmatrix} X_1(t) & X_2(t) \end{pmatrix}^T$.

Now:

$$X(t) = X(0) + R_1(t)\begin{pmatrix} -1 \\ 1 \end{pmatrix} + R_2(t)\begin{pmatrix} 1 \\ -1 \end{pmatrix}$$

The counting processes R_1 and R_2 are represented as unit-rate Poisson processes. A unit-rate Poisson process can be constructed considering:

- $\{e_i\}_{i=1}^{\infty}$ independent exponential random variables with a parameter of 1.
- $\tau = e_1, \tau_2 = \tau_1 + e_2, \ldots, \tau_n = \tau_{n-1} + e_n$.

The associated unit-rate Poisson processes $Y(s)$ is the counting process determined by the number of points $\{\tau_i\}_{i=1}^{\infty}$ that come before $s \geq 0$. Let $\lambda : [0,\infty[\to \mathbb{R}_{\geq 0}$ be the rate of movement along the time axis, then the number of points observed by time s is:

$$Y\left(\int_0^s \lambda(r)\,dr\right)$$

From the basic properties of exponential random variables, whenever $\lambda(s) > 0$, the probability of seeing a jump within the next small increment of time Δs is:

$$P\left(Y\left(\int_0^{s+\Delta s} \lambda(r)\,dr\right) - Y\left(\int_0^s \lambda(r)\,dr\right) \geq 1\right) \sim \lambda(s)\Delta s$$

Thus the propensity for seeing another jump is $\lambda(s)$. Noting that $\forall s, X_1(s) + X_2(s) = 1$, the propensity for reactions 1 and 2 are:

$$\lambda_1(X(s)) = \alpha X_1(s), \quad \lambda_2(X(s)) = \beta X_2(s)$$

Combining all of the above R_1 and R_2 can be represented as:

$$R_1(t) = Y_1\left(\int_o^t \alpha X_1(s)\,ds\right), \quad Y_2\left(\int_0^t \beta X_2(s)\,ds\right)$$

So a pathways representation for the stochastic model can be obtained:

$$X(t) = X_0 + Y_1\left(\int_0^t \alpha X_1(s)\,ds\right)\begin{pmatrix} -1 \\ 1 \end{pmatrix} + \\ + Y_2\left(\int_o^t \beta X_2(s)\,ds\right)\begin{pmatrix} 1 \\ -1 \end{pmatrix}$$

Where Y_1 and Y_2 are independent, unit-rate Poisson processes. Suppose now that $X_1(0) + X_2(0) = N \geq 1$. The model is focusing on the number of open and closed ion channels out of a total of N. Suppose that the propensity at which ion channels are opening can be modelled as:

$$\lambda_1(t, X(t)) = \alpha(t) X_1(t)$$

And the rate at which they close:

$$\lambda_2(t, X(t)) = \beta(t) X_2(t)$$

Where $\alpha(t)$ and $\beta(t)$ are non-negative functions of time, probably depending on voltage. Suppose that for each $i \in \{1,2\}$, the conditional probability of seeing the counting process R_1 increase in the interval $[t, t+h[$ is $\lambda_1(t, X(t))h + o(h)$. The expression is now:

$$X(t) = X_0 + Y_1\left(\int_0^t \alpha(s) X_1(s)\,ds\right)\begin{pmatrix} -1 \\ 1 \end{pmatrix} + \\ + Y_2\left(\int_0^t \beta(s) X_2(s)\,ds\right)\begin{pmatrix} 1 \\ -1 \end{pmatrix}$$

A jumping model consisting of d chemical constituents (ion channel states) undergoing transitions determined via $M > 0$ different reaction channels. Moreover suppose that $X_i(t)$ determines the value of the ith constituent at time t, so that $X(t) \in \mathbb{Z}^d$, that the propensity function for the kth reaction is $\lambda_k(t, X(t))$ and that if the kth reaction channel takes place at time t, then the system is updated according to the addition of the reaction vector $\zeta_k \in \mathbb{Z}^d$:

$$X(t) = X(t-) + \zeta_k$$

The path-wise stochastic representation for the model is:

$$X(t) = X_0 + \sum_k Y_k\left(\int_0^t \lambda_k(s, X(s))\,ds\right)\zeta_k$$

Where Y_k are independent unit-rate Poisson processes. The chemical master equation is:

$$\frac{d}{dt} = \sum_{k=1}^{M} P_{X_0}(x-\zeta_k,t)\lambda(t,x-\zeta_k) + \\ - P_{X_0}(x,t)\sum_{k=1}^{M}\lambda_k(t,x)$$

Where $P_{X_0}(x,t)$ is the probability of being in state $x \in \mathbb{Z}^d_{\geq 0}$ at time $t \geq 0$ given an initial condition of X_0.

When X represents the randomly fluctuating state of an ion channel in a single compartment conductance based neuronal model, the membrane potential $V \in \mathbb{R}$ is added as an additional dynamical variable. The voltage is considered to evolve deterministically, conditional on the states of the ion channels. Suppose that there is a single ion channel type with state variable X, then the pathwise representation is supplemented with the solution of Kirchoff's current conservation law:

$$C\frac{dV}{dt} = I_{app}(t) - I_V(V(t)) - \left(\sum_{i=1}^{d} g_i^o X_i(t)\right)(V(t)-V_X)$$

Where:

- g_i^o is the conductance of an individual channel in the ith state.
- The sum gives the total conductance associated with the channel represented by the vector X.
- The reversal potential is V_X.
- $I_V(V)$ captures deterministic voltage-dependent currents due to other channels.
- I_{app} is a time-varying, deterministic applied current.

The propensity function will be a function of the voltage, so $\lambda_k(s,X(s))$ will be replaced with $\lambda_k(V(s),X(s))$. If there are a finite number of types of channels, the vector $X \in \mathbb{Z}^d$ represents the aggregated channel state.

2.1.1 Simulation of the representation

This representation implies a simulation strategy in which each point of the Poisson processes Y_k denoted τ_n is generated sequentially as needed. So the time until the next reaction that occurs past time T is:

$$\Delta = \min_k \left\{ \Delta_k : \int_0^{T+\Delta_k} \lambda_k(s,X(s))ds = \tau_T^k \right\}$$

Where τ_T^k is the first point associated with Y_k coming after $\int_0^T \lambda_k(s,X(s))ds$:

$$\tau_T^k = \inf\left\{ r > \int_0^T \lambda_k(s,X(s))ds : \right. \\ \left. Y_k(r) - Y_k\left(\int_0^T \lambda_k(s,X(s))ds\right) = 1 \right\}$$

The reaction that took place is the index at which the minimum is achieved. This allows to write the algorithm 1.

Algorithm 1: `RandomTimeChangeSimulation()`

X = Initial number of molecules of each species
V = Initial voltage
$t = 0$
$T = 0$
foreach k **do**
  $\tau_k = 0$
  $T_k = 0$
$\{r_k\} = [\cdots]$
for $i = 0$ **to** M **do**
  $r_k[i] = norm(0,1)$
  $\tau_k = \ln\left(\frac{1}{r_k}\right)$
while $T < T_{\max}$ **do**
  $\Delta = 0$
  while $\int_t^{t+\Delta} \lambda_k(V(s),X(s))ds \neq \tau_k - T_k$ **do**
    Integrate forward in time: $C\frac{dV}{dt} = I_{app}(t) - I_V(V(t)) - \left(\sum_{i=1}^{d} g_i^o X_i(t)\right)(V(t)-V_X)$
    $\Delta += \Delta t$
  $\mu = k$ such that $\int_t^{t+\Delta} \lambda_k(V(s),X(s))ds\tau_k - T_k$
  foreach k **do**
    $T_k = T_k + \int_t^{t+\Delta} \lambda_k(V(s),X(s))ds$
  $t += \Delta$
  $X \leftarrow X + \zeta_\mu$
  $r = norm(0,1)$
  $\tau_\mu += \ln\left(\frac{1}{r}\right)$
  $T = T + t$
return to the while or quit

In this algorithm T_k denotes the value of the integrated intensity function $\int_0^t \lambda_k(s,X(s))ds$ and τ_k the first point associated with Y_k located after T_k. All random number are assumed to be independent. With a probability of one, the index μ is unique at each step. This algorithm also relies on being able to compute a hitting time for each of the $T_k(t) = \int_0^t \lambda_k(s,X(s))ds$ exactly, which is in general not possible, but it will be sufficient with reliable integration software. If the equations for the voltage or the intensity functions can be analytically solved, such numerical integration is unnecessary and efficiencies can be gained.

2.2 Gillespie representation

The Gillespie representation is an alternative representation for the stochastic process built before. Let:

- Y be a unit rate Poisson process.

- $\{\epsilon_i, i = 0, 1, 2, \dots\}$ be independent, uniform $(0, 1)$ random variables independent of Y.

  Set:

$$\lambda_0(V(s), X(s)) = \sum_{k=1}^{M} \lambda_k(V(s), X(s))$$

$$q_0 = 0$$

  And $\forall k \in \{1, \dots, M\}$:

$$q_k(s) = \lambda_0(V(s), X(s))^{-1} \sum_{l=1}^{k} \lambda_l(V(s), X(s))$$

  Where X and Y satisfy:

$$R_0(t) = Y\left(\int_o^t \lambda_0(V(s), X(s))ds\right)$$

$$X(t) = X(0) + \sum_{k=1}^{M} \zeta_k \int_0^t 1\{\epsilon_{r_0(s-)} \in [q_{k-1}(s-), q_k(s-)[\} dR_0(s)$$

$$C\frac{dV}{dt} = i_{app}(t) - I_V(V(t)) - \left(\sum_{i=1}^{d} g_o^o X_i(t)\right)(V(t) - V_X)$$

The stochastic process (X, V) descried in the equation above is a Markov process equivalent to the one described in the previous section. To understand it note that $R_0(t)$ determines the holding time in each state and the middle equation determines the embedded discrete time Markov chain or skeletal chain in the usual manner. This is the representation for the Gillespie algorithm, with time dependent propensity functions. This representation is analogous to the PDMP formalism with λ_0 the rate function that determines the time of the next jump and the middle equation the transitions.

2.2.1 Simulation of the representation

The simulation is analogous of using Gillespie's algorithm in the time-homogeneous case. The algorithm is 2 and all number are assumed to be independent.

This algorithm also relies on being able to compute a hitting time.

Algorithm 2: `GillespieRepresentation()`

```
X = Initial number of molecules of each species
V = Initial voltage
t = 0
T = 0
while T < T_max do
    r = norm(0, 1)
    while ∫_t^{t+Δ} λ_0(V(s), X(s)) ds ≠ ln(1/r) do
        Integrate forward in time: C dV/dt = I_app(t) −
          I_V(V(t)) − (Σ_{i=1}^{d} g_i^o X_i(t))(V(t) − V_X)
        Δ+ = Δt
    ϵ = norm(0, 1)
    Δ_1 = 0
    k_1 = 0 foreach k do
        if ϵ ∈ [q_{k−1}((t + Δ)−), q_k((t + Δ)−)] then
            Δ_1 = Δ
            k_1 = k
    t+ = Δ_i
    X ← X + ζ_{k_1}
    T+ = t
```

3. Morris-Lecar

The Morris-Lecar system is a concrete illustration of the exact stochastic simulation algorithms. It was developed as a model for oscillation observed in barnacle muscle fibers. The determinist equations constitute a planar model for the evolution of the membrane potential $v(t)$ and the fraction of potassium gates $n \in [0, 1]$ that are in the open state. In addition to this there is a depolarizing current gated by a rapidly equilibrating variable m, the calcium conductance which is treated now as a fast, deterministic variable as in the standard fast/slow decomposition or the planar Morris-Lecar model. The mean field equation for this model are:

$$\frac{dv}{dt} = f(v, n) = \frac{1}{C}(I_{app} - g_{Ca} m_\infty(v)(v - v_{Ca}) + - g_L(v - v_L) - g_K n(v - v_K))$$

$$\frac{dn}{dt} = g(v, n) = \alpha(v)(1 - n) - \beta(v)n = \frac{n_\infty(v) - n}{\tau(v)}$$

The kinetics of the potassium channel can be specified by the instantaneous time constant τ, the asymptotic target n_∞ or by the per capita transition rates α and β. Moreover:

$$m_\infty = \frac{1}{2}\left(1 + \tanh\left(\frac{v - v_a}{v_b}\right)\right)$$

$$\alpha(v) = \frac{\phi \cosh\left(\frac{\epsilon}{2}\right)}{1 + e^{2\epsilon}}$$

$$\beta(v) = \frac{\phi \cosh\left(\frac{\epsilon}{2}\right)}{1 + e^{-2\epsilon}}$$

$$n_\infty(v) = \frac{\alpha(v)}{\alpha(v) + \beta(v)} = \frac{1 + \tanh \epsilon}{2}$$

$$\tau(v) = \frac{1}{\alpha(v) + \beta(v)} = \frac{1}{\phi \cosh \frac{\epsilon}{2}}$$

Where $\epsilon = \frac{v - v_c}{v_d}$ and the parameter will have values:

- $v_K = -84.$
- $v_L = -60.$
- $v_{Ca} = 120.$
- $I_{app} = 100.$
- $g_K = 8.$
- $g_L = 2.$
- $C = 20.$
- $v_a = -1.2.$
- $v_b = 18.$
- $v_c = 2.$
- $v_d = 30.$
- $\phi = 0.04.$
- $g_{Ca} = 4.4.$

For which the deterministic system has a stable limit cycle. For smaller values of the applied currents the system has a stable fixed point that loses stability through a subcritical Hopf bifurcation as I_{app} increases.

3.1 Deterministic model

Before applying the two representation presented we implemented the Morris Lecar as a fully deterministic system abstracting from the single channel processes and using the asymptotic value m_∞. The behaviour of the model can be seen in figure 5.

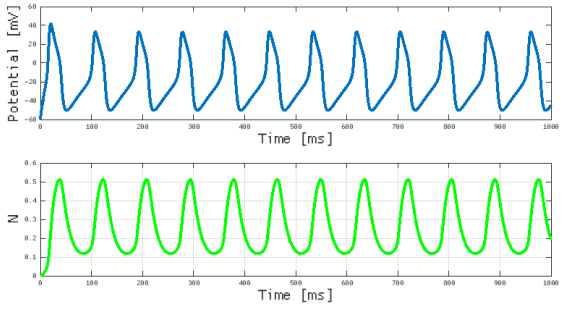

Figure 5. Implementation of the fully deterministic Morris Lecar model. **TOP** Membrane potential. **Bottom** Fraction of open potassium channel.

3.2 Stochastic model

A finite number of potassium channels N_{tot} is introduced and the number of open channels are treated as a discrete random process. Each potassium channel switches between the closed or open state independently of the other with voltage-dependent per capita transition rates α and β. The entire population conductance ranges from 0 to $g_K^o = \frac{g_K}{N_{tot}}$. In this simulation $N_{tot} = 40$. The random variables will be the voltage and the number of open potassium channel. In the random time change representation the opening and closing of the potassium channels are driven by two independent unit rate Poisson processes $Y_{open}(t)$ and $Y_{close}(t)$. The evolutions of V and N are linked. Whenever $N = n$, the evolution of V obeys a deterministic differential equation:

$$\left.\frac{dV}{dt}\right|_{N=n} = f(V, n)$$

N evolves as a jump process: $N(t)$ is a piece-wise constant, with transitions occurring with intensities dependent on V. Whenever $V = v$:

$$N \to N + 1 \text{ net rate } \alpha(v)(N_{tot} - N)$$

$$N \to N - 1 \text{ net rate } \beta(v)N$$

Now representing the state space for N graphically:

$$0 \underset{\beta}{\overset{\alpha N_{tot}}{\rightleftarrows}} 1 \underset{2\beta}{\overset{\alpha(N_{tot}-1)}{\rightleftarrows}} 2 \underset{3\beta}{\overset{\alpha(N_{tot}-2)}{\rightleftarrows}} \cdots \underset{k\beta}{\overset{\alpha(N_{tot}-k+1)}{\rightleftarrows}} k$$

$$\alpha(N_{tot}-k)\downarrow\uparrow(k+1)\beta$$

$$N_{tot} \underset{N_{tot}\beta}{\overset{\alpha}{\rightleftarrows}} (N_{tot}-1) \underset{\beta(N_{tot}-1)}{\overset{2\alpha}{\rightleftarrows}} \cdots \underset{(k+2)\beta}{\overset{\alpha(N_{tot}-k-1)}{\rightleftarrows}} (k+1)$$

The nodes represent possible states for process N an the transition intensities located above and below the arrows. Adopting the random time change representation the stochastic Morris-Lecar system is written as:

$$\begin{aligned}\frac{dV}{dt} =& f(V(t), N(t)) = \\ =& \frac{1}{C}(I_{app} - g_{Ca} m_\infty(V(t))(V(t) - V_{Ca}) - g_L(V - V_L) + \\ & - g_K^o N(t)(V(t) - V_K))\end{aligned}$$

$$\begin{aligned}N(t) = N(0) &- Y_{close}\left(\int_0^t \beta(V(s))N(s)ds\right) + \\ & Y_{open}\left(\int_0^t \alpha(V(s))(N_{tot} - N(s))ds\right)\end{aligned}$$

3.2.1 Random time change representation

We simulated the stochastic Morris Lecar model considering only the Potassium channel through the random time change representation for 4000 seconds. The relationship within voltage and the number of open channel can be seen in figure 6.

3.2.2 Gillespie's representation

We simulated the stochastic Morris Lecar model considering only the Potassium channel through Gillespie's representation for 4000 seconds. The relationship within voltage and the number of open channel can be seen in figure 7.

4. Models with more than one channel type

Now the original Morris-Lecar model is considered, where there is a three-dimensional phase space. In the original treatment of voltage oscillations in barnacle muscle fibres the calcium gating variable m is included as a dynamical variable, sot the total system is describes with the following deterministic equations:

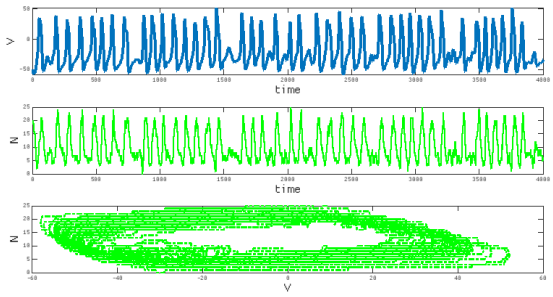

Figure 6. The Morris Lecar stochastic model with only potassium channels. From top to bottom: **1** The membrane voltage. **2** The number of open potassium channel over time. **3** The number of open potassium channels over voltage.

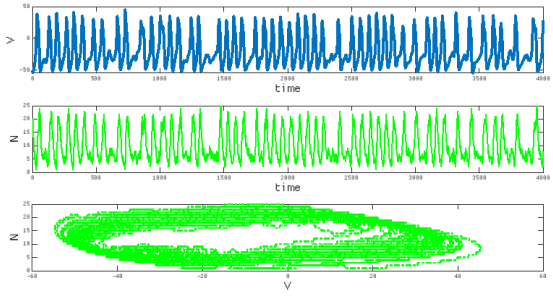

Figure 7. The Morris Lecar stochastic model with only potassium channels. From top to bottom: **1** The membrane voltage. **2** The number of open potassium channel over time. **3** The number of open potassium channels over voltage.

$$\frac{dv}{dt} = F(v,n,m) = \frac{1}{C}(I_{app} - g_L(v - v_L) + \\ - g_{Ca}m(v - v_C a) - g_K n(v - v_K))$$

$$\frac{dn}{dt} = G(v,n,m) = \alpha_n(v)(1-n) - \beta_n(v)n = \\ = \frac{n_\infty(v) - n}{\tau_n(v)}$$

$$\frac{dm}{dt} = H(v,n,m) = \alpha_m(v)(1-m) - \beta_m(v)m = \\ = \frac{m_\infty(v) - m}{\tau_m(v)}$$

The number of calcium gates evolves according to this equation instead of being set to its asymptotic value $m_\infty = \frac{\alpha_m}{\alpha_m + \beta_m}$. The planar form of the equation is obtained by observing that m approaches equilibrium faster than n and v, so using standard arguments from singular perturbation theory this system can be brought into the planar model by replacing F and G with: $f(v,n) = F(v,n,m_\infty(v))$ and $g(v,n) = G(v,n,m_\infty(v))$. Now for the $3D$ model $\epsilon_m = \frac{v - v_a}{v_b}$ has to be introduced in addition to $\epsilon_n = \frac{v - v_c}{v_d}$. It can be noted how ϵ_x represents where the voltage falls along the activation curve for channel type x, relative to its half-activation point (v_a for calcium and v_c for potassium)and its slope (reciprocals of v_b for calcium and v_d for potassium). The per capita opening and closing rates for each channel type are then:

$$\alpha_m(v) = \frac{\phi_m \cosh\frac{\epsilon_m}{2}}{1 + e^{2\epsilon_m}} \quad \beta_m(v) = \frac{\phi_m \cosh\frac{\epsilon_m}{2}}{1 + e^{-2\epsilon_m}}$$

$$\alpha_n(v) = \frac{\phi_n \cosh\frac{\epsilon_n}{2}}{1 + e^{2\epsilon_n}} \quad \beta_n(v) = \frac{\phi_n \cosh\frac{\epsilon_n}{2}}{1 + e^{-2\epsilon_n}}$$

With parameters:

- $v_a = -1.2$.
- $v_b = 18$.
- $v_c = 2$.
- $v_d = 30$.
- $\phi_m = 0.4$.
- $\phi_n = 0.04$

The asymptotic open probabilities are given by m_∞ and n_∞ and the time constants τ_m and τ_n, which satisfy the relations:

$$m_\infty(v) = \frac{\alpha_m(v)}{\alpha_m(v) + \beta_m(v)} = \frac{1 + \tanh\epsilon_m}{2}$$

$$n_\infty(v) = \frac{\alpha_n(v)}{\alpha_n(v) + \beta_n(v)} = \frac{1 + \tanh\epsilon_n}{2}$$

$$\tau_m(v) = \frac{1}{\phi\cosh\frac{\epsilon_m}{2}}$$

$$\tau_n(v) = \frac{1}{\phi \cosh \frac{\epsilon_n}{2}}$$

Assuming a population of M_{tot} calcium and N_{tot} potassium gates a stochastic hybrid system is obtained, with a continuous variable $V(t)$ and two discrete ones $M(t)$ and $N(t)$. The voltage evolves according to the sum of the applied, leak, calcium and potassium currents

$$\begin{aligned}\frac{dV}{dt} = & F(V(t), N(t), M(t)) = \\ = & \frac{1}{C}\Big(I_{app} - g_L(V(t) - v_L) - g_{Ca}\frac{M(t)}{M_{tot}}(V(t) - v_{Ca}) + \\ & - g_K\frac{N(t)}{N_{tot}}(V(t) - v_K)\Big)\end{aligned}$$

The number of open gates change only by unit increases and decreases remaining constant between such changes. So the channel states evolve according to:

$$\begin{aligned}M(t) = & M(0) - Y^M_{close}\left(\int_0^t \beta_m(V(s))M(s)ds\right) + \\ & + Y^M_{open}\left(\int_0^t \alpha_m(V(s))(M_{tot} - M(s))ds\right)\end{aligned}$$

$$\begin{aligned}N(t) = & N(0) - Y^N_{close}\left(\int_0^t \beta_n(V(s))N(s)ds\right) + \\ & + Y^N_{open}\left(\int_0^t \alpha_n(V(s))(N_{tot} - N(s))ds\right)\end{aligned}$$

4.1 Deterministic representation

Firstly we analysed the trajectory of the fully deterministic model, which can be seen in figure 8.

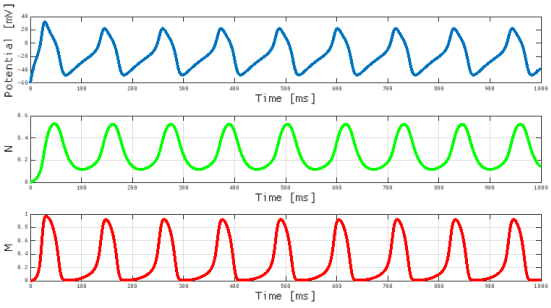

Figure 8. Deterministic Morris Lecar model with evolving potassium and calcium dynamics. From top to bottom: **1** Membrane voltage. **2** Fraction of open potassium channels. **3** Fraction of open calcium channels.

4.2 Random time change representation

We simulated the stochastic Morris Lecar model through the random time change representation for 4000 seconds. The relationship within voltage and the number of open channel can be seen in figure 9.

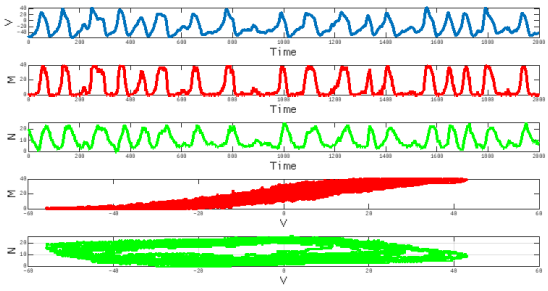

Figure 9. The Morris Lecar stochastic model with only potassium channels. From top to bottom: **1** The membrane voltage. **2** The number of open calcium channel over time. **3** The number of open potassium channels over time. **4** The number of open calcium channel over voltage. **5** The number of open potassium channel over voltage

4.3 Gillespie's representation

We simulated the stochastic Morris Lecar model through Gillespie's representation for 4000 seconds. The relationship within voltage and the number of open channel can be seen in figure 10.

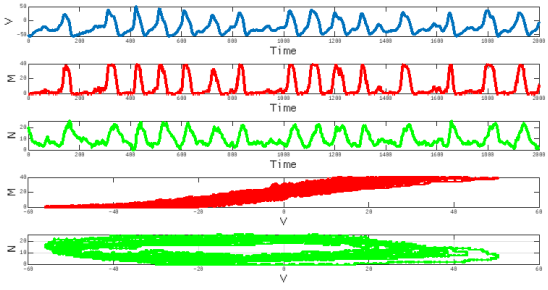

Figure 10. The Morris Lecar stochastic model with only potassium channels. From top to bottom: **1** The membrane voltage. **2** The number of open calcium channel over time. **3** The number of open potassium channels over time. **4** The number of open calcium channel over voltage. **5** The number of open potassium channel over voltage

5. Comparison of the exact algorithm with a piecewise constant propensity approximation

The most common implementation for hybrid ion channel models is an approximate method in which the per capita reaction propensities are held fixed between channel events: in particular in algorithm 1, $\int_t^{t+\Delta k} \lambda_k(V(s), X(s))ds$ is replaced with $\Delta_k \lambda_k(V(t), X(t))$, leaving the remainder unchanged. In this type of algorithms the sequence of channel states jumps is generated using the propensity immediately following the most recent jump rather than taking into account the time dependence of the reaction propensities due to the changing voltage. This is analogous to the forward Euler method for the numerical solution of ordinary differential equations. The solution of a stochastic differential equation with a given initial condition is a map from the sample space Ω to a space

of trajectories. In this context Ω is one independent unit rate Poisson process per reaction channel. For the planar model a point in Ω amounts to fixing two Poisson process, Y_{open} and Y_{closed} to drive the transitions of the potassium channels. For the full 3D model there are four processes:

- $Y_1 \equiv Y_{Ca,open}$.
- $Y_2 \equiv Y_{Ca,closed}$.
- $Y_3 \equiv Y_{K,open}$.
- $Y_4 \equiv Y_{K,closed}$.

The exact algorithm provides a numerical solution of the map from $\{Y_k\}_{k=1}^4 \in \Omega$ and initial conditions (M_0, N_0, V_0) to the trajectory $(M(t), N(t), V(t))$. The approximate piecewise algorithm gives a map from the same domain to a different trajectory $(\tilde{M}(t), \tilde{N}(t), \tilde{V}(t)$. To make a pathways comparison the initial condition and the four Poisson processes are fixed and the resulting trajectories are compared. Both algorithms produce a sequence of noise-dependent voltage spike with similar firing rates. The two trajectories remain close together initially and the timing for the first spike is similar for both. Over time discrepancies between the trajectories accumulate: the timing of the second and third spikes is different and before ten spikes the spike trains have become uncorrelated. Even though the trajectories diverge the two processes could still generate sample paths with similar time-dependent or stationary distributions: the two algorithms could still be close in a weak sense. Given M_{tot} and N_{tot} the density for the hybrid Markov process can be written as:

$$\rho_{m,n}(v,t) = \frac{1}{dv} Pr\{M(t) = m, N(t) = n, V \in [v, v+dv]\}$$

Obeying the master equation:

$$\begin{aligned}\frac{\partial \rho_{m,n}(v,t)}{\partial t} =& -\frac{\partial (F(v,n,m)\rho_{m,n}(v,t))}{\partial v} + \\ &- (\alpha_m(v)(M_{tot}-m) + \beta_m(v)m + \\ &+ \alpha_n(v)\cdot(N_{tot}-m) + \beta_n(v)n)\rho_{m,n}(v,t) + \\ &+ (M_{tot}-m+1)\alpha_m(v)\rho_{m-1,n}(v,t) + \\ &+ (m+1)\beta_m(v)\rho_{m+1,n}(v,t) + \\ &+ (N_{tot}-n+1)\alpha_n(v)\rho_{m,n-1}(v,t) + \\ &+ (n+1)\beta_n(v)\rho_{m,n+1}(v,t)\end{aligned}$$

With initial condition $\rho_{m,n}(v,0) \geq 0$ given by any integrable density such that $\in_{v\in\mathbb{R}} \sum_{m,n} \rho_{m,n}(v,0)dv \equiv 1$ and boundary conditions:$\rho \to 0$ as $|v| \to \infty$ and $\rho \equiv 0$ for either $m, n < 0$ or $m > M_{tot}$ or $n > N_{tot}$. The approximate algorithm does not generate a Markov process since the transition probabilities depend on the past rather than the present value of the voltage. Because of this they do not satisfy the master equation, but it is plausible that they may have a unique stationary distributoin.

Looking the histograms in the (v, n) plane with entries summed over m. The algorithms were run with independent randomm number streams in the limit cycle regime ($I_{app} = 100$) fir $I_{max} \approx 200000$ time units, sampled every 10. Considering $N_{tot} = M_{tot} = k$, for $k < 5$ the difference is obvious, while increasing k the histograms become more and more similar.

Looking now at bar plots of the histograms with points projected on the voltage axis: entries summed over m and n, the plots become increasingly similar the greater the $k>$

To quantify the similarity of the histogram the empirical L_1 difference between them has been computed. For the full (v, n, m) histograms and then for the collapsed voltage axis. Let $\rho_{m,n}(v)$ and $\tilde{\rho}_{m,n}(v)$ denote the stationary distributions for the exact and approximate algorithms respectively. To compare the two the L_1 distance between them is approximated:

$$d(\rho, \tilde{\rho}) = \int_{v_{\min}}^{v\max} \left(\sum_{m=0}^{M_{tot}} \sum_{n=0}^{N_{tot}} |\rho_{m,n}(v) - \tilde{\rho}_{m,n}(v)| \right) dv$$

Where v_{min} and v_{max} where chosen so that $F(v_{min}, n, m > 0 \wedge F(v_{max}, n, m) < 0 \forall m, n$. Such value must exist since $F(v, n, m)$ is linear and monotonically decreasing for v for any fixed pair of (n, m). For any exact simulation algorithm, once the voltage component falls between $v_{min} \leq v \leq v_{max}$ it remains in that interval for all time.

6. Coupling, variance reduction and parametric sensitivities

The random time change formalism can be used to develop new and faster computational methods with no loss in accuracy coupling two processes in order to reduce the variance and increase the speed of different natural estimatore. Consider for example the computation of parametric sensitivities, which is a tool that allow to determine parameters to which a system output is most responsive. Suppose that the intensity or propensity functions are dependent on some vectors of parameters θ. θ may represent a subset of the system's mass action kinetics constants, the cell capacitance, or the underlying number of channels of each type. To know how sensitively a quantity such as the average firing rate or interspike interval variance depends on θ a family of models (V^θ, X^θ), parameeterized by θ is considered, with stochastic equations:

$$\frac{d}{dt} V^\theta(t) = f(\theta, V^\theta(t), X^\theta(t))$$

$$X^\theta(t) = x_0^\theta + \sum_k Y_k \left(\int_0^t \lambda_k^\theta(V^\theta(s), X^\theta(s))ds \right) \zeta_k$$

Where f is some function and all other notation is as before. Some quantities depend on the entire sample path. Let $g(\theta, V^\theta, X^\theta)$ be a path functional capturing the quantity of interest. In order to evaluate the relative

shift in expectation of g due to a perturbation of the parameter vector, the estimation would be:

$$\tilde{s} = \epsilon^{-1}\mathbb{E}\big[g(\theta', V^{\theta'}, X^{\theta'}) - g(\theta, V^{\theta}, X^{\theta})\big] \approx$$
$$\approx \frac{1}{\epsilon N}\sum_{i=1}^{N}\big[g(\theta', V^{\theta'}_{[i]}, X^{\theta'}_{[i]}) - g(\theta, V^{\theta}_{[i]}, X^{\theta}_{[i]})\big]$$

Where:

- $\epsilon = ||\theta - \theta'||$.
- $(V^{\theta}_{[i]}, X^{\theta}_{[i]})$ is the ith path generated with parameter θ.
- N is the number of sample paths computed for the estimation.

A finite difference and Monte Carlo sampling could be used to approximate the change in expectation. If the paths $(V^{\theta'}_{[i]}, X^{\theta'}_{[i]})$ and $(V^{\theta}_{[i]}, X^{\theta}_{[i]})$ are generated independently, the variance of the estimator for $\tilde{s}$ is $O(N^{-1}\epsilon^{-2})$ and its standard deviation $O(N^{-\frac{1}{2}}\epsilon^{-1})$. In order to reduce the confidence interval of the estimator to a target level of $\rho > 0$:

$$N^{-\frac{1}{2}}\epsilon^{-1} \lesssim \rho \Rightarrow N \gtrsim \epsilon^{-2}\rho^{-2}$$

Which can be prohibitive. Reducing the variance of the estimator can be achieved coupling the processes $(V^{\theta'}_{[i]}, X^{\theta'}_{[i]})$ and $(V^{\theta}_{[i]}, X^{\theta}_{[i]})$ so that they are correlated by constructing them on the same probability space. Different approach to this problem are discussed in the next sections.

6.1 The common random number method

The common random number CRN method simulates bot processes according to Gillespie representation with the same Poisson process Y and the same stream of random variables $\{\epsilon_i\}$.

6.2 The common reaction path method

The common reaction path method CRP simulates both processes according to the same random time change representation with the same Poisson processes Y_k. One stream of uniform random variables for each reaction channel is created and used for the simulation of both processes.

6.3 The coupled finite difference method

The coupled finite difference method CFD utilizes a split coupling method. It splits the counting process for each of the reaction channels into three pieces:

- One counting process shared by X^{θ} and $X^{\theta'}$ and has propensity equal to the minimum of their respective intensities.
- One that only accounts for the jumps of X^{θ}.
- One than only accounts for the jumps of $X^{\theta'}$.

Letting $a \wedge b = \min\{a, b\}$, the precise coupling is:

$$X^{\theta'}(t) = X^{\theta'}_0 + \sum_k Y_{k,1}\left(\int_0^t m_k(\theta, \theta', s)ds\right)\zeta_k +$$
$$+ \sum_k Y_{k,2}\left(\int_o^t \lambda^{\theta'}_k(V^{\theta'}(s), X^{\theta'}(s)) - m_k(\theta, \theta', s)ds\right)\zeta_k$$

$$X^{\theta}(t) = X^{\theta}(t) + \sum_l Y_{k,1}\left(\int_0^t m_k(\theta, \theta', s)ds\right)\zeta_k +$$
$$+ \sum_k Y_{k,3}\left(\int_0^t \lambda^{0}_k(V^{\theta}(s), X^{\theta}(s)) - m_k(\theta, \theta', s)ds\right)\zeta_k$$

Where:

$$m_k(\theta, \theta', s) = \lambda^0_k(V^{\theta}(s), X^{\theta}(s)) \wedge \lambda^{\theta'}_k(V^{\theta'}(s), X^{\theta'}(s))$$

And $\{Y_{k,1}, Y_{k,2}, Y_{k,3}\}$ are independent unit-rate Poisson processes.

6.4 Covariance and methods' performace

The algorithm presented could still produce statistically equivalent path. This is not the case for the methods for parametric sensitivities provided. Each of the methods constructs a coupled pair of processes $((V^{\theta'}_{[i]}, X^{\theta'}_{[i]}), (V^{\theta}_{[i]}, X^{\theta}_{[i]}))$ and the marginal processes $(V^{\theta'}_{[i]}, X^{\theta'}_{[i]})$ and $(V^{\theta}_{[i]}, X^{\theta}_{[i]})$ are all statistically equivalent no matter the method used. The covariance $Cov((V^{\theta'}_{[i]}, X^{\theta'}_{[i]}), (V^{\theta}_{[i]}, X^{\theta}_{[i]}))$ can be different. This is important since the objective is the variance reduction for any component X_j:

$$Var(X^{\theta}_k(t) - X^{\theta'}_j(t)) = Var(X^{\theta}_j(t)) + Var(X^{\theta'}_k(t)) - 2Cov(X^{\theta}_j(t), X^{\theta}_j$$

Minimizing the variance is equivalent to maximizing the covariance. The CRN method is the worst at maximizing covariance. The CFD method with the split coupling procedure is the best, though the CRP method can be more efficient in some context.

7. Discussion

The random time change representation can be useful to computational neuroscience as it allows for generalization of computational methods developed in the context of biochemistry, in which the propensities depend upon the state of the jump process only, so that variance reduction strategies become feasible. The random time change approach avoids several approximations: for example in simulation algorithms based on a fixed time step chemical Langevin approach, it is necessary to assume that the increments in channel state are Gaussian distributed over an

appropriate time interval. However in exact simulation of small patches the exact algorithm visits states incompatible with the Gaussian increment approximation regardless of time step size. Another algorithm found in literature is the piecewise constant propensity or approximate forward algorithm. This ignore changes to membrane potential during the intervals between channel state changes. As the sensitivity of ion channel opening and closing to voltage is fundamental these algorithm are not appropriate unless time between openings and closing is especially small. This study restrict attention to the suprathreshold regime of the Morris-Lecar model, in which the applied current puts the system above the Hoph bifurcation marking onset of oscillations. Spiking is not the result of noise-facilitated release. Another study used eigenfunction expansion methods, path integrals and theory of large deviations to study spike initiation as noise facilitated escape problem in the excitable regime, as well as to incorporate synaptic currents into a stochastic network model using versions of the exact algorithm presented in this paper. the usual separation-of-time scales picture breaks done: the firing rate obtained by 1D Kramers rate theory when the slow recovery variable (fraction of open potassium channels) is taken to be fixed does not match that obtained by direct simulation with the exact algorithm. By considering a maximum likelihood approach to the 2D escape problem, spontaneous closure of potassium channels contributes significantly to noise induced escape than spontaneous opening of sodium channel. The algorithm presented are applicable beyond the effects of channel noise on the regularity of action potential firing in a single compartment neuron model. Exact simulation of hybrid stochastic models have been used to study spontaneous dendritic NMDA spikes, intracellular growth of the T7 bacteriophage and hybrid stochastic network models taking into account piecewise deterministic synaptic currents. The latter example represents a significant extension of the neural master equation approach to stochastic population models. The random time change representation extends naturally to scenarios in which each channel has a greater number of states, but it would be better to combine it with complexity reduction methods such as the stochastic shielding algorithm. Analysis of algorithms combining stochastic shielding and the random time change framework are a promising direction for future research.

References

[1] Integrate and fire model generation. https://www.cns.nyu.edu/~david/handouts/integrate-and-fire.pdf.

[2] L. Harrison, O. David, and K. Friston. Stochastic models of neuronal dynamics. *Philosophical Transactions of the Royal Society B: Biological Sciences*, 360(1457):1075–1091, 2005.